Indian Journal of Geo Marine Sciences
Vol. 54 (09), September 2025, pp. 441-451
DOI: 10.56042/ijms.v54i09.18333

Research Article

Uniqueness of discharge coefficient of sluice passage for tidal power plant: CFD modelling

J-S Jo*[,a] & K-S Kim[b]

[a]Faculty of Earth and Environmental Sciences, Kim Il Sung University, Ryongnam-Dong, Taesong-District, Pyongyang, Democratic People's Republic of Korea

[b]Department of Architectural Science, State Academy of Sciences, Ryonmot-Dong, Sosong-District, Pyongyang, Democratic People's Republic of Korea

*[E-mail: js.jo@ryongnamsan.edu.kp]

Received 28 March 2025; revised 22 July 2025

The discharge coefficient (C_d) of the sluice passage in tidal power plants is an important index targeted by many tidal power studies aiming to improve the discharge capability of the sluice passage and, thus, the efficiency of tidal power generation. In this work, the discharge capability of the two most common types of sluice passages (*i.e.*, Venturi- and culvert-type passages) was analysed and compared through the Computational Fluid Dynamics (CFD) simulations using Flow 3D. The results of this study clearly demonstrated the uniqueness of the discharge coefficient *i.e.*, the C_d values estimated for each of the Venturi and culvert passages were constant irrespective of the position of cross sections selected along the passage. Most importantly, unlike previous results, the C_d values estimated at the throat and outlet sections for the Venturi passage were the same. The mean C_d values for the Venturi and culvert passages were about 0.8 and 0.91, respectively, with maximum relative differences of 4.9 % and 3.2 %, respectively, indicating superior discharge capability of the culvert passage over the Venturi one. It is believed that the present results will help researchers and engineers accurately estimate and improve the discharge capability of sluice passages for tidal power plants.

[**Keywords**: CFD, Discharge coefficient, Sluice passage, Tidal power plant, Uniqueness]

Introduction

With the issues of global warming and climate change, the world's energy strategy is turning towards renewable energy sources, such as wind, solar, and ocean energy[1]. In particular, the large amount of electricity generated by tidal barrages or lagoons makes them an attractive renewable energy option[2,3]. The theoretical tidal range resource in the United Kingdom was reported to exceed 25 GW, accounting for 50 % of the tidal resource available in Europe[4]. At present, a few tidal power plants, such as Jiang Xia (China), Annapolis (Canada), and La Rance (France), have been operating worldwide[1]. In the Democratic People's Republic (DPR) of Korea, the Taedong tidal power scheme feasibility study has been underway for almost 10 years[5].

Many hydraulic structures, including sluice and turbine passages, ship locks and embankments, can be placed for the tidal power barrage[6]. Especially, the sluice passage where a vertical sluice gate or radial gate could be housed is among the important structures that significantly affect the amount of electricity generated from the tidal power barrage, because well-designed passages allow more water for generating electricity[7].

Estimating the flow characteristics through sluice gate is considered as a major issue in hydraulic engineering and of theoretical and practical significance. The flows under sluice gates have been extensively studied by many engineers and researchers, focusing on estimating the discharge coefficient (C_d)[8–13]. The flow condition of sluice gates can be distinguished as either a free flow, a partially submerged flow, or a fully submerged flow[14–16]. As early as 1950, Henry[8] performed a series of lab experiments to determine the range of C_d for a vertical sluice gate. From the experimental results, a relationship between the C_d value and the ratio of upstream water depth to gate opening y_1/w was proposed for free and submerged flows, providing a well-known nomograph of this relationship. The several relationships based on Henry's nomograph[8] were suggested by Swamee[9] to determine C_d for free and submerged flows in sluice gates. In 2011, Habibzadeh *et al.*[17] performed a theoretical analysis based on the Energy–Momentum (EM) method to obtain a relationship for C_d of sluice gates for free and submerged flows in rectangular channels. Although the energy losses are neglected in most studies of sluice gates, Habibzadeh *et al.*[17] showed that for the submerged flows, turbulence can cause significant energy losses. They introduced an energy-loss factor (k) presented as a function of the gate geometry, and showed that it affects the discharge coefficient. In Sauida[10], a general equation for C_d was derived from the multiple regression of the experimental data. The results indicated that asymmetric operation of multi-sluice gates and increasing the expansion ratio yield higher C_d values. Artificial Neural Network (ANN) was modelled with the back-propagation learning algorithm to determine C_d of vertical and inclined sluice gates for both free and submerged flows[11]. Kubrak *et al.*[12] used Swamee's model[9] as a basis for determining C_d from the experimental data. The influences of sills with different geometries on the flow through sluice gates were studied experimentally and numerically by Daneshfaraz *et al.*[13]. They suggested that the Renormalization-Group (RNG) turbulence model shows higher accuracy than the k - ε, k - ω, and Large Eddy Simulation (LES) turbulence models. Furthermore, the C_d value of sluice gates with various sill states was higher than that of the no-sill state. Recently, Yoosefdoost & Lubitz[16] analysed and simplified some models to improve their accuracy and applicability in the design of sluice gates. In their study, new equations and methods were proposed to estimate C_d for EM considering energy losses (EML) and Hydrologic Engineering Centers River Analysis System (HEC-RAS) models. They showed that for the volumetric flow rate and C_d, the accuracy of EM, EML, and Henry's models for free flow and EM and EML models for submerged flow was reasonable. In general, as described above, the sluice gate models have been well studied and documented.

By contrast, despite their importance, there has been little literature on estimating and improving the flow rate and discharge coefficient through sluice passages. Most importantly, it should be noted that although the sluice gates are housed in sluice passages, the discharge capability of sluice passages is generally estimated without considering sluice gates (*i.e.*, under the condition that the sluice gates are fully opened)[6,18]. Hydraulic tests were carried out to propose an improved sluice passage design for the Severn Barrage[18]. In their study, careful attention to passageway designs led to a high discharge capability. Baker[6] suggested that a developed Venturi-type passage design with a gently curved inlet showed superior discharge capability compared to a classic one based on the Dall tube shape. Most recently, the Computational Fluid Dynamics (CFD) modelling results showed that a culvert-type passage had superior discharge capability compared to a Venturi-type one when the outlet area of the two passages was the same[5].

Meanwhile, because of the particular geometrical shape of the Venturi-type sluice passage (*i.e.*, a long passage with varying cross-sectional area) and the lack of research on its discharge capability, there are still important issues to be solved. Baker[6], often cited in previous studies on tidal power plants[2,4,19–22], suggested that for the Venturi-type passage, the C_d values obtained at the throat and outlet sections differ. In the literature, during the flood tide, the C_d values at the throat and outlet are estimated to be 1.65 and 0.91, respectively for the classic Venturi design, but 1.8 and 0.87, respectively for the Severn design. From Baker[6], it is indicated that for any one Venturi-type passage, a lot of C_d values can be obtained, because the cross-sectional areas of the passage are different. However, to the best of our knowledge, the discharge capability of sluice passages (especially Venturi-type passages) needs to be investigated in more detail.

In this context, this study aims to demonstrate the uniqueness of the discharge coefficient for any one sluice passage numerically, *i.e.*, the C_d values estimated for the sluice passage are constant irrespective of the position of cross sections selected along the passage. In other words, it is demonstrated from this study that the C_d values obtained at the throat and outlet sections of one sluice passage (especially a Venturi-type passage) are the same.

Materials and Methods

In the present study, the CFD modelling generally included the following steps: building the 3D computational model using SOLIDWORKS and exporting in the file format (stl), importing the STL file into the Flow 3D, building the mesh of the computational domain, defining the flow, initial and boundary conditions, and then running the CFD model. The additional steps, such as error analysis against experimental data, mesh sensitivity analysis, and testing of turbulence models, were also included to ensure successful numerical simulation runs. The results (*i.e.*, water levels, velocities, pressures) obtained from numerical simulations were used to determine the discharge coefficient of sluice passages using the discharge coefficient equation.

Discharge coefficient equation

As described in the Supplementary Data, the C_d value at the throat section (or any passage cross-section) of the passage can be calculated as follows:

$$C_d = \frac{Q}{A_t\sqrt{2g\Delta h_t}} \quad \ldots (1)$$

Where, Q is the flow rate through the sluice passage (m^3/s), g is the gravitational acceleration (= 9.8 m/s^2), A_t is the flow area (m^2) at the throat (or any passage cross section), and Δh_t is the head difference (m) between the upstream and throat (or any passage cross section) defined as:

$$\Delta h_t = \left(h_u + \frac{p_u}{\rho g} + \frac{V_u^2}{2g}\right) - \left(h_t + \frac{p_t}{\rho g}\right) \quad \ldots (2)$$

Where, h_u is the mean water level (m) at the upstream section, p_u is the pressure (Pa) at the upstream (= the atmospheric pressure, p_{atm}), ρ is the density of water (kg/m^3), V_u is the mean flow velocity (m/s) at the upstream, h_t is the water level (m) at the throat or any cross section of the passage (the height of the ceiling, *i.e.*, inner upper wall, at the selected section), p_t is the pressure (Pa) at the ceiling ($\neq p_{atm}$) of the selected section.

The C_d value at the outlet section of the passage can be calculated as follows:

$$C_d = \frac{Q}{A_e\sqrt{2g\Delta h_e}} \quad \ldots (3)$$

Where, A_e is the flow area (m^2) at the outlet. Because $p_t = p_{atm}$ at the outlet, the head difference (m), Δh_e, between the upstream and outlet sections is defined as follows:

$$\Delta h_e = \left(h_u + \frac{V_u^2}{2g}\right) - h_d \quad \ldots (4)$$

Where, h_d is the mean water level immediately downstream from the passage.

From Eqs. (1) and (2), it is indicated that for a Venturi-type passage, the areas (A_t), water levels (h_t) and pressures (p_t) of the passage cross section required for calculating the discharge coefficient can greatly differ depending on which cross section of the passage is chosen. Furthermore, as shown in Eqs. (2) and (4), when calculating C_d at throat and outlet sections, the head difference equations required are significantly different.

Geometry construction

For this study, the two main types of passages (*i.e.*, Venturi and culvert) used in the feasibility study for the Taedong tidal power plant[5] were created in SOLIDWORKS 2016 software. Figure 1 shows the plan, side, and 3D views of the two passage models used in the present study. These two passage models had the same length (31 m) and the same inlet and outlet areas (168 m^2, *i.e.*, width × height = 14 m × 12 m). For the Venturi passage (Fig. 1a), the throat area was 100 m^2 (10 m × 10 m) and the passage cross-sectional areas were different, while for the culvert passage (Fig. 1b), the cross-sectional area of the passage was constant (*i.e.*, 168 m^2).

Governing equations

To demonstrate the uniqueness of the discharge coefficient of sluice passages, numerical simulations were carried out using the CFD software Flow 3D version 11.2. In this numerical model, the flow fields in Cartesian coordinates were modelled by solving the Reynolds-Averaged Navier–Stokes (RANS) equations and the RNG k - ε turbulence model. Among

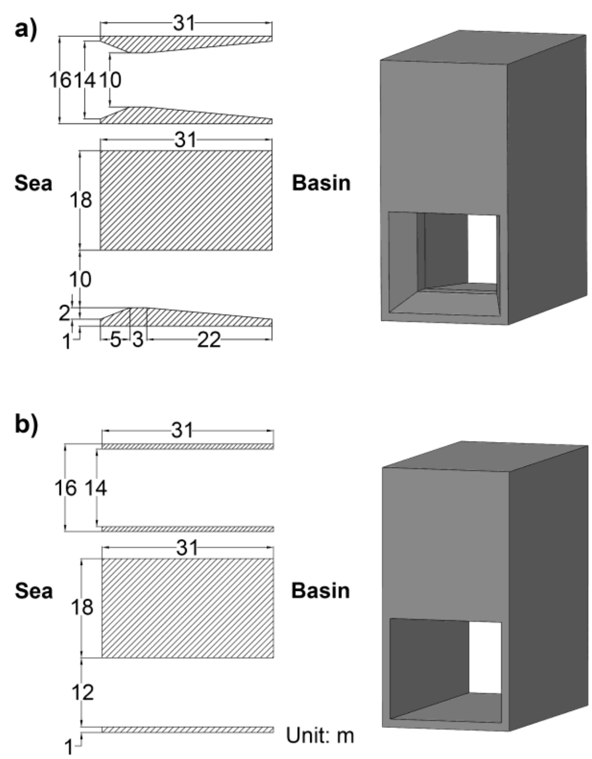

Fig. 1 — Plan, side, and 3D views of (a) Venturi-, and (b) Culvert-type passage models used in the present study

turbulence models, the RNG k - ε model represents the flow characteristics near the solid wall with a higher accuracy than other turbulence models, such as the k - ε model[23–25], which is also shown in the Subsection "Mesh sensitivity analysis and validation". The Volume Of Fluid (VOF) technique was used to track the interface between air and water (*i.e.*, the free surface). Details of the governing equations, the RNG k - ε turbulence model, and the VOF scheme used in this study can be found in the literature[25,26].

Mesh generation and boundary conditions

For numerical simulations, the open-channel models with sluice passages were also created in SOLIDWORKS 2016. To avoid the water level oscillations by surface eddies near the sluice passage, the size of the open channel models (*i.e*., computational domain) must be large enough. Especially, acceptable flow conditions (*i.e*., fully developed flow) in the streamwise (x) direction generally require long upstream and downstream lengths of open channel preceding and following the sluice passage. Furthermore, the long upstream and downstream lengths were required to reproduce the conditions of the experimental flume used in the present study. Useful background information for setting up the upstream and downstream lengths can be found in the literature[5,27] and references cited therein. For the above reasons, the size of the computational domain was set to 531 m in the x-direction, 16 m in the y-direction, and 31 m in the z-direction for all the simulation cases (Fig. 2a). In other words, the width of the channel bed (B) was almost equal to that of the passage inlet (B_t), *i.e*., $B / B_t = 1$. The bottom length of the apron section was set to 20 m. The horizontal length of the apron slope was 20 m, which corresponded to 5 times the vertical length of the apron slope (4 m) – that is, the apron slope (S) was set to 1:5 in this study.

Meanwhile, the final mesh was obtained through the mesh sensitivity study with the experimental data, as explained in the Subsection "Mesh sensitivity analysis and validation". Based on the mesh sensitivity analysis, the mesh sizes were set between 0.25 and 0.5 m in the x-direction (0.25 m near the passage), while in the y and z-directions, the uniform mesh size of 0.5 m was used (Fig. 2b). As a result, a total of 3,495,808 mesh cells were generated. The simulations were performed with the four different discharge rates (Q = 300, 400, 500, and 600 m^3/s) at a constant h_u of 16 m.

For the computational domain, the solid walls of the passage and the two $x – z$ lateral boundary planes have a no-slip boundary condition (Fig. 3). The volume flow rate condition was imposed on the inlet plane (*i.e.*, the $y – z$ beginning plane), while the outlet plane (*i.e.*, the $y – z$ end plane) was given as an outflow boundary condition. Due to the use of the VOF scheme to track the free surface, constant atmospheric pressure and zero shear stress were applied as boundary conditions at the air-water interface, as described in Hirt & Nichols[28]. The frictional effects along the solid surface were considered by taking the surface roughness.

Numerical simulation

The density and dynamic viscosity of the working fluid (seawater in this study) were set to ρ = 1,025 kg/m^3 and $\mu = 1.22\times10^{-3}$ Pa s, respectively. The maximum time step (Δt) was 0.01 s, while the

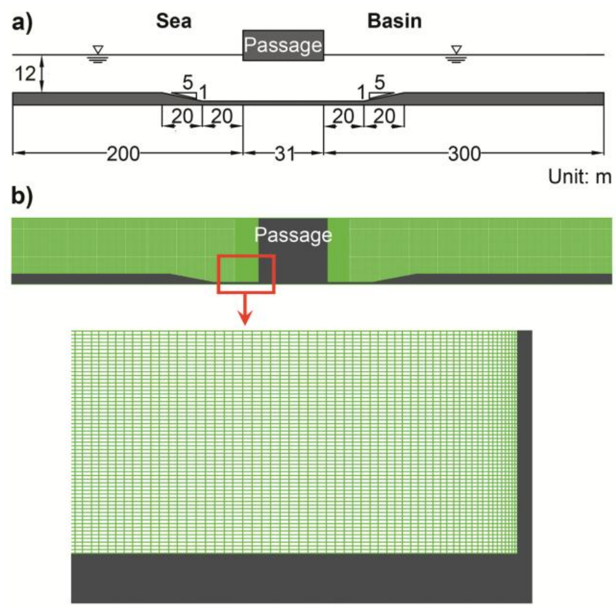

Fig. 2 — (a) Schematic layout of the open channel with the culvert passage, and (b) Computational domain gridding

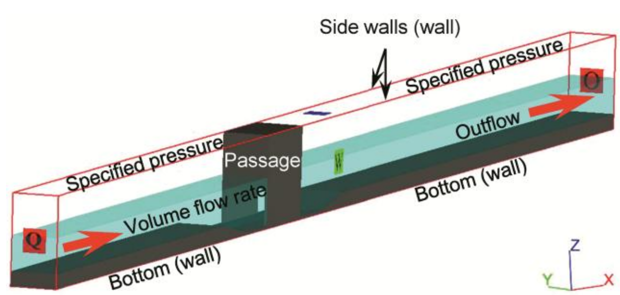

Fig. 3 — Boundary conditions defined for the computational domain used in this study

computational time for all the simulation cases was set to 1,500 s. Once steady-state flow regimes were fully established, the data obtained were used to assess the discharge capacity of sluice passage models.

In order to demonstrate the uniqueness of the discharge coefficient, the measurement points taken along the Venturi and culvert sluice passages are shown in Figure 4. For each passage, the measuring points were distributed along the centerline of the passage, with a total of 16 points at intervals of 2 m (except the 15th interval of 3 m, *i.e.*, between points 15 and 16). For the Venturi and culvert passages, the flow cross-sectional areas at the measurement points are listed in Table 1.

The present study used only Eqs. (1) and (2) to demonstrate the uniqueness of the discharge coefficient of Venturi and culvert passages numerically, because Eqs. (3) and (4) can be used only at the outlet section. All simulations in this study were conducted on the HP BladeSystem C7000 (HP BL460c) owned by Kim Il Sung University, the DPR Korea.

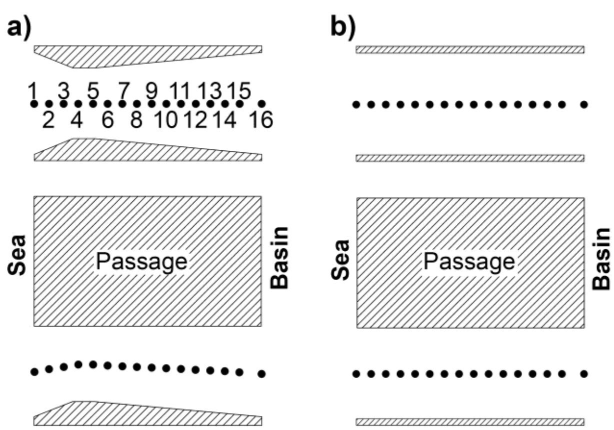

Fig. 4 — Plan and side views of (a) Venturi-, and (b) Culvert-type passages with measurement points

Experimental setup

First, the validation of the 3D CFD model was performed by comparing numerical and experimental results. The passage models for the physical experiment were based on the prototype passages (*i.e.*, Fig. 1). Large-scale physical modelling experiments indicated that Reynolds number may affect the flow fields through the passage, but the primary forces governing the flow behaviour in these regions are gravity and inertia[18]. For flows driven by inertia and gravity forces, it is clear that the Froude scaling law is applicable, as reported in separate studies[29–31]. Their results indicated that Reynolds number effects were not significant in these situations at these scales. Based on the Froude similarity law and considering the laboratory conditions for the present study, the physical model with a scale of 1/60 was made, which was still enough to prevent the effects of Reynolds number and surface tension from becoming significant[18]. In this study, the scale effects under the Froude similitude were described in the Subsection “Mesh sensitivity analysis and validation”. The physical experiments were performed in a rectangular glass flume measuring 15 m long, 0.3 m wide, and 0.9 m high (Fig. 5). The passage models were installed about 6 m from the flume inlet. The plexiglass was used as a material for making the passage models, because the surface roughness of the reduced-scale physical model made of this material was considered to adequate for reproducing that of the prototype sluice passage made of concrete. Additional details, including the experimental setups and measuring methods, are described in the literature[5] and in paper (Kim & Jo, 2024) cited therein. Based on the Froude similarity law, the length, width, and height of the open channel were set to 13.3, 0.4, and 0.8 m, respectively. Meanwhile, the experimental conditions Q were 0.0296, 0.0395, 0.0494, and 0.0593 m^3/s at a constant h_u of 0.4 m. To compare the

Table 1 — Flow cross-sectional areas (m^2) at the measurement points along the passages

Point number	Flow cross-sectional area (m^2)		Point number	Flow cross-sectional area (m^2)	
	Venturi	Culvert		Venturi	Culvert
1	168	168	9	122	168
2	139	168	10	128	168
3	112	168	11	133	168
4	100	168	12	139	168
5	100	168	13	146	168
6	105	168	14	152	168
7	111	168	15	158	168
8	116	168	16	168	168

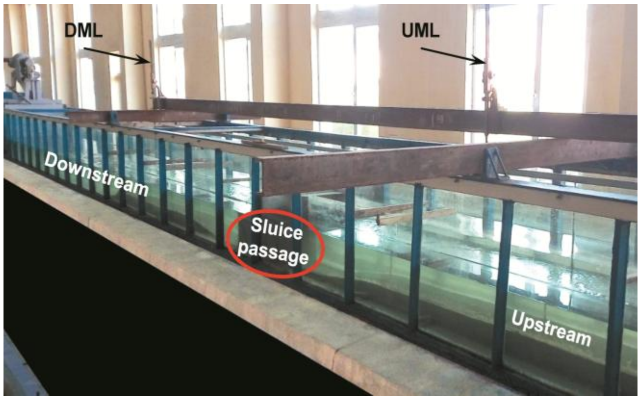

Fig. 5 — Photograph of the rectangular glass flume used for the laboratory experiment in this study. UML and DML indicate the upstream and downstream measurement locations

results of the laboratory experiment and CFD modelling, the water levels, velocities, and pressures measured in the physical experiment were inversely scaled to those of the actual field conditions of the prototype (*i.e.*, the numerical conditions in this study) by using the scale of 1/60 based on the Froude scaling law. The general flowchart for determining the discharge coefficient of sluice passages in this study is shown in Figure 6.

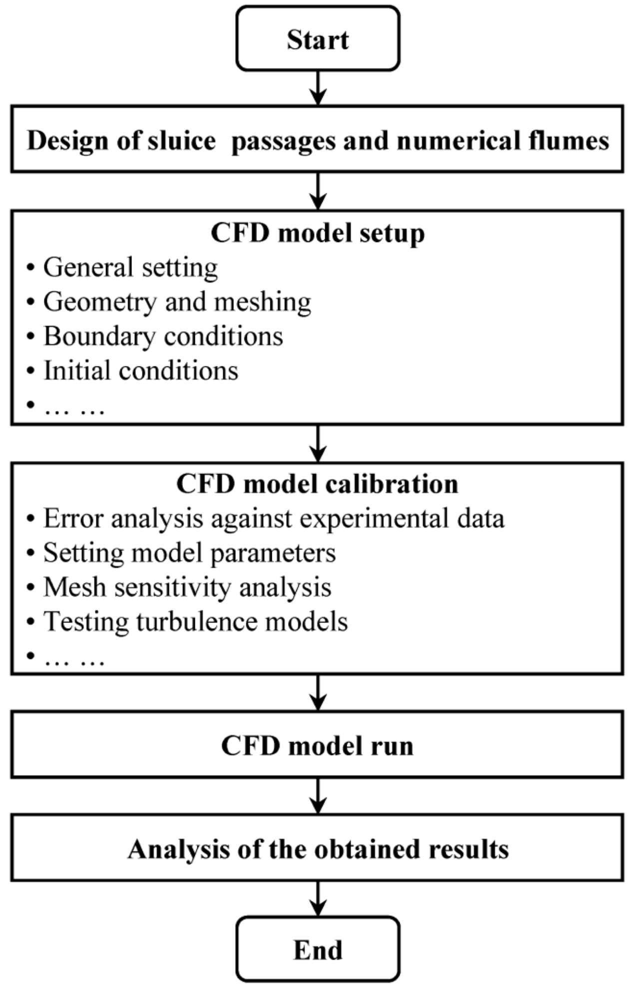

Fig. 6 — Schematic flowchart for determining the discharge coefficient of sluice passages in this study

Simulation Results

Mesh sensitivity analysis and validation

As described above, the mesh sensitivity test was carried out to select the adequate mesh resolution for the CFD modelling in this study. The entire computational domain was meshed at five different resolutions to select the optimal mesh that yielded a converged solution, reasonable computational time, and accurate results. For the Venturi- and culvert-type passages, the head difference (Δh_e) between the upstream and downstream sections was used to compare the simulated values for different mesh sizes. The number of mesh cells varied from 263,376 (for Mesh-1) to 13,983,232 (for Mesh-5) (Table S1). It should be noted that for Mesh-3, Mesh-4, and Mesh-5, the mesh sizes were set between 0.25 and 0.5 m in the *x*-direction (0.25 m near the passage). It is clear from Tables S1 and S2 that as the mesh resolution improved, the relative error between the simulated value for each mesh and the measured value decreased significantly, whereas the computational time increased significantly. The simulated Δh_e values using Mesh-5 were the finest for both the Venturi- and culvert-type passages. However, in the case of Mesh-5, the computational times were the longest. Generally, among the mesh resolutions considered in this study, Mesh-3, Mesh-4, and Mesh-5 had better results than the first two mesh resolutions, and their simulations were reasonable (less than 6 % relative error). Importantly, there was no significant improvement in the simulated results between Mesh-3 and Mesh-5. Therefore, Mesh-3 was used in the present study, because it simulated the head difference more accurately than Mesh-4 and Mesh-5, with less computational time.

Three different "two-equation" turbulence models available in Flow 3D, such as standard $k - \varepsilon$, RNG $k - \varepsilon$, and $k - \omega$, were tested to simulate the turbulence effects of the water flow through the sluice passages (Table S3). Mesh-3 was used to estimate the performance of turbulence models. As shown in Table S3, the RNG $k - \varepsilon$ model was generally better than the other two models in simulating the head difference, and the standard $k - \varepsilon$ model showed the worst performance. Generally, the above results suggested that the CFD modelling using the RNG $k - \varepsilon$ turbulence model and Mesh-3 was reliable for estimating the flow characteristics of the sluice passages in this study.

When the same fluid, water herein, under the Froude similitude is used in both the laboratory model and the prototype, the Reynolds number in the laboratory model is substantially underestimated[32]. In other words, it is impossible to keep both the Reynolds and Froude numbers in the laboratory model and prototype. Practically, an important rule in physical modelling is that the Reynolds number of the physical model should be as large as possible, so that if the flow condition of the prototype is turbulent, the flow condition of the physical model is turbulent. In this case, the Reynolds number range must be Re > 1×10^3 to 5×10^3, as described in the literature[33]. Table S4 shows the Reynolds and Froude numbers at the upstream section under the conditions of Q = 0.0296, 0.0395, 0.0494, and 0.0593 m^3/s (300, 400, 500, and 600 m^3/s in the prototype, respectively) for the laboratory model (Venturi-type passage). As shown in Table S4, the Reynolds numbers were greater than 7×10^4 for the four different discharge rates, which satisfied the Reynolds scaling criterion[33]. When Q = 0.0593 m^3/s, the Froude numbers were 0.187, 0.486, and 0.193 at the upstream, throat, and downstream sections, respectively, indicating that the state of flow in this study was considered subcritical[34]. Furthermore, the Froude numbers were nearly identical between the laboratory model and the prototype (*i.e.*, the numerical model in this study), satisfying the Froude scaling criterion. The ranges of the Froude and Reynolds numbers for the culvert-type passage were similar to those of the Venturi one.

Flow patterns around sluice passages

Figure 7 shows several typical streamlines in the *xz*-planes inside the passages during steady flow. As shown in Figure 7, for the culvert passage, the streamlines were nearly parallel to the top wall, whereas for the Venturi passage, they were not. Furthermore, the closer to the bottom wall of the Venturi passage, the more curved the streamlines, whereas the closer to the bottom wall of the culvert passage, the straighter the streamlines. From Figure 7, it is clear that the streamlines and the centerline for each of the Venturi and culvert passages were geometrically similar.

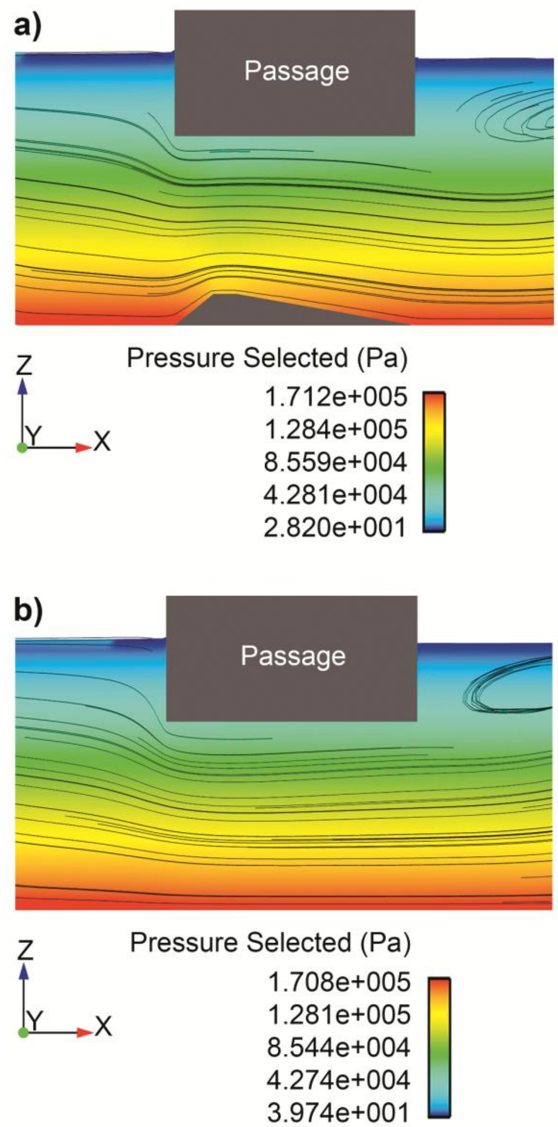

Fig. 7 — Side views of the streamlines inside the (a) Venturi-, and (b) Culvert-type passage models

Discharge coefficient of sluice passages

Figure 8 shows the mean C_d values obtained at 16 measurement points along the centerline of the Venturi passage. The mean C_d values obtained along the centerline of the Venturi passage were about 0.8 (Fig. 8). The maximum relative difference of the simulated C_d values was about 4.9 %.

Figure 9 shows the variation in the C_d values according to the head difference (Δh_t) at the throat (the fourth point in the *x*-direction) of the Venturi passage for Q = 300, 400, 500, and 600 m^3/s. The maximum relative difference in the values of C_d according to Δh_t was about 1.47 %, as shown in Figure 9, indicating that the influence of Δh_t on C_d is negligible.

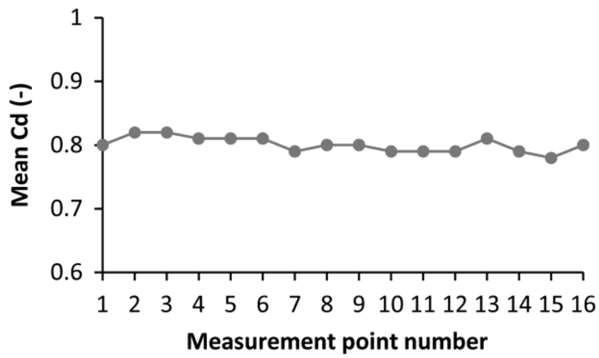

Fig. 8 — Mean C_d values obtained at the measurement points of the Venturi-type passage

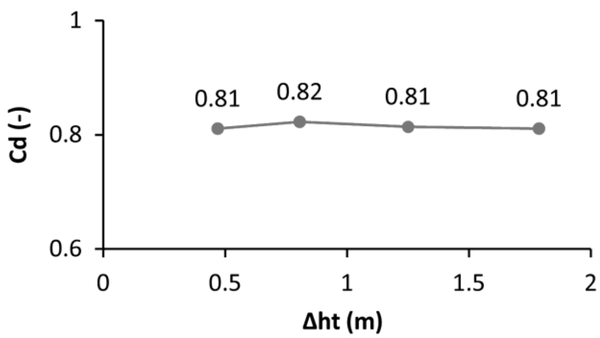

Fig. 9 — Variation in the C_d values according to Δh_t

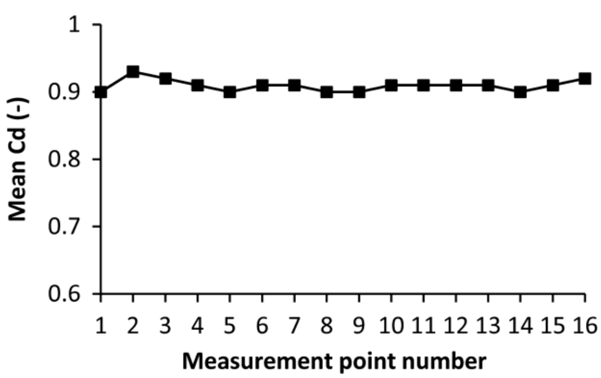

Fig. 10 — Mean C_d values obtained at the measurement points of the culvert-type passage

Figure 10 illustrates the mean C_d values obtained at 16 measurement points along the centerline of the culvert passage for the four discharge rates. The results for the culvert passage showed almost the same trend as those for the Venturi passage (Fig. 10). The mean C_d values at measurement points along the centerline of the culvert passage were about 0.91. For the culvert passage, the maximum relative difference in the C_d simulated values was about 3.2 %. From Figures 8 and 10, it is clear that the discharge capacity of the culvert-type passage was about 13.6 % higher than that of the Venturi one.

Discussion

The present study aimed to demonstrate the uniqueness of the discharge coefficient of sluice passages for tidal power plant numerically.

First of all, the study clearly showed that the estimated C_d values were constant along each of the considered Venturi- and culvert-type passages. In other words, it was demonstrated from the present results that for each of the Venturi- and culvert-type passages, the C_d values obtained at the throat and outlet sections were the same. However, in Baker[6], the C_d value for one Venturi-type passage was found to be different at the throat and outlet sections. It is guessed that in the previous study, the same discharge equation (more exactly, the same head difference equation) was used, regardless of whether the throat or outlet section was considered. As a result, for one Venturi-type passage, the C_d value obtained at the throat section was always larger than that at the outlet one, because the throat area was always smaller than the outlet one. In other words, the C_d values at the throat and outlet sections were as different as the ratio of the throat area to the outlet one. For example, for the Severn design, the C_d value at the throat section was more than twice as large as that at the outlet one. From Eqs. (1) to (4), it is clear that the discharge equations (especially the head difference equations) to be used at the throat and outlet sections of Venturi-type passage are significantly different. For the case of calculating the C_d value at any passage cross section (including the throat section), the pressure at the cross section must be considered. In the present study, the maximum relative errors of the simulated C_d values for the Venturi- and culvert-type passages were very small (4.9 % and 3.2 %, respectively).

Secondly, this study also demonstrated that the culvert-type passage has a superior discharge capability compared to the Venturi-type passage when the outlet area of the two passages is the same. In such a case, similar results showing higher discharge capacity for culvert-type passages can be found in Jo & Kim[5]. Previous studies have reported that the C_d value of the Venturi-type passage is higher than that of the culvert-type passage, showing a higher water flow rate under the condition that their throat areas are the same. For this reason, Venturi-type sluice passages have attracted special attention from many engineers and researchers for a long time[6,18]. However, Jo & Kim[5] suggested that, under the condition that the outlet area, but not the throat area, of the Venturi and culvert passages is the same, evaluating, comparing, and improving their discharge capability would be of practical significance. For this condition, the culvert passage shows a higher discharge capacity than the Venturi one, as demonstrated by the results of this study.

Finally, the present results showed that the C_d values of sluice passages were less than 1. Strictly speaking, the discharge coefficient is theoretically expressed as the ratio of the real flow rate to the ideal one, as described in the Supplementary Data. That is, $C_d = Q_{real} / Q_{ideal}$. Therefore, the C_d value must be less than 1 under actual flow conditions. Typical example results can be found in previous studies on estimating the discharge coefficient of vertical sluice gates or radial gates. From the well-known Henry's (1950) nomograph[8], it can be seen that the C_d value was highest (0.611) in the free-flow condition, whereas it decreased in the submerged-flow regimes. For sluice gates, some studies suggested using C_d as 0.6, and the HEC-RAS model typically suggested $0.5 \leq C_d \leq 0.7$, as discussed in the literature[16]. Habibzadeh *et al.*[17] proposed neglecting the energy loss resulted in an overestimation of C_d by approximately 5 %. From their study, it is recognised that the value of the energy-loss factor (k) is a function of the sluice gate geometry and can affect the C_d value for both free and submerged flows. The C_d values were 0.590 and 0.563, respectively, for k = 0.0 and 0.1 in the free-flow condition. Sauida[10] showed that C_d varied from 0.58 to 0.8 for different expansion ratios (e). The values of C_d for different positions of the sill were 0.779, 0.731, and 0.686, respectively[13]. It is shown that for the submerged flow regime, the calibrated C_d (i.e., 0.363) was significantly lower than the minimum value of C_d proposed by the HEC-RAS model[16]. In previous studies[6] concerning the discharge capability of sluice passages for tidal power plants, the C_d values were estimated to exceed 1, especially at the throat section of the Venturi-type passage. The present results clearly showed that regardless of the type of the passage, the C_d value obtained at any cross-section of the passage was less than 1.

Conclusion

A better understanding of the flow characteristics of sluice passages for tidal power plants is of theoretical and practical significance. In this study, the uniqueness of the discharge coefficient of sluice passages for a tidal power plant was numerically demonstrated. The results of this study showed that the C_d value of any one sluice passage was the same at all sections of the passage. Furthermore, this study demonstrated that the culvert passage had superior discharge capability than the Venturi one under the same outlet area. The major limitation of the present study is that different surface roughness conditions on the inner walls of sluice passages were not considered, which can increase the difficulty and complexity of demonstrating the uniqueness of discharge capability by causing turbulence. The Venturi-type passages with different geometries were not used, which was also a limitation of this study. For the Venturi-type passages, the sudden contraction and expansion of the flow cross-sectional area can significantly affect their discharge coefficient, which needs to be clarified in future studies. The influence of the passage length on the discharge coefficient will also require further investigation, because this effect is very important in narrow and long flow passages, such as pipes, ducts and siphons, as well as sluice passages. In general, it is recognised that the C_d value of sluice passages can be affected by many hydraulic and structural conditions; therefore, recommending a typical range of C_d is one of the difficult tasks for engineers and researchers. There are still important knowledge gaps relevant to the discharge coefficient of sluice passages, in comparison with the sluice gates. Therefore, further studies will help engineers and researchers fully understand the discharge capability of sluice passages, and it is believed that this study can provide insight into future research directions to resolve such problems.

Supplementary Data

Supplementary data associated with this article is available in the electronic form at https://nopr.niscpr.res.in/jinfo/ijms/IJMS_54(09)441-451_SupplData.pdf

Acknowledgments

Authors thank the State Hydro-Meteorological Administration (SHMA) of the DPR Korea for help received to perform the CFD simulations. This study has been supported by a feasibility study project for the construction of tidal power plants in the DPR Korea.

Funding

The authors received no financial support for the research, authorship, and/or publication of this paper.

Conflict of interest

The authors declare that they have no conflict of interest.

Author Contributions

J-SJ: Conceptualization, methodology, project administration, supervision, and writing, review and editing; and K-SK: Formal analysis, software, visualisation, and writing original draft. Both the authors reviewed and approved the final manuscript.

References

1 Waters S & Aggidis G, Tidal range technologies and state of the art in review, *Renew Sustain Energy Rev*, 59 (2016) 514–529. http://dx.doi.org/10.1016/j.rser.2015.12.347

2 Xia J, Falconer R A & Lin B, Impact of different tidal renewable energy projects on the hydrodynamic processes in the Severn Estuary, UK, *Ocean Model*, 32 (1–2) (2010) 86–104. http://dx.doi.org/10.1016/j.ocemod.2009.11.002

3 Mackinnon K, Smith H C M, Moore F, van der Weijde A H & Lazakis I, Environmental interactions of tidal lagoons: A comparison of industry perspectives, *Renew Energy*, 119 (2018) 309–319. https://doi.org/10.1016/j.renene.2017.11.066

4 Bray S, Ahmadian R & Falconer R A, Impact of representation of hydraulic structures in modelling a Severn barrage, *Comput Geosci*, 89 (2016) 96–106. http://dx.doi.org/10.1016/j.cageo.2016.01.010

5 Jo J – S & Kim K – S, A choice of sluice passage for a tidal power plant: Venturi- or culvert-type passage? *Proc Instit Civ Eng – Energy*, 178 (3) (2025) 122–132. https://doi.org/10.1680/jener.23.00069

6 Baker A C, *Tidal Power*, (The Institute of Engineering and Technology, London), 2006, pp. 250.

7 Xia J Q, Falconer R A, Lin B L & Tan G M, Estimation of annual energy output from a tidal barrage using two different methods, *Appl Energy*, 93 (2012) 327–336. http://dx.doi.org/10.1016/j.apenergy.2011.12.049

8 Henry H R, Discussion: 'Diffusion of submerged jet', *Trans Am Soc Civ Eng*, 115 (1950) 687–694.

9 Swamee P, Sluice gate discharge equations, *J Irrig Drain Eng*, 118 (1) (1992) 56–60. http://doi.org/10.1061/(ASCE)0733-9437(1992)118:1(56)

10 Sauida M F, Calibration of submerged multi-sluice gates, *Alexandria Eng J*, 53 (3) (2014) 663–668. http://dx.doi.org/10.1016/j.aej.2014.04.008

11 Rady R A E H, Modeling of flow characteristics beneath vertical and inclined sluice gates using artificial neural networks, *Ain Shams Eng J*, 7 (2) (2016) 917–924. http://dx.doi.org/10.1016/j.asej.2016.01.009

12 Kubrak E, Kubrak J, Kiczko A & Kubrak M, Flow measurements using a sluice gate; Analysis of applicability, *Water*, 12 (3) (2020) p. 819. http://dx.doi.org/10.3390/w12030819

13 Daneshfaraz R, Norouzi R, Abbaszadeh H, Kuriqi A & Di Francesco S, Influence of Sill on the Hydraulic Regime in Sluice Gates: An Experimental and Numerical Analysis, *Fluids*, 7 (2022) p. 244. https://doi.org/10.3390/fluids7070244

14 Belaud G, Cassan L & Baume J-P, Calculation of contraction coefficient under sluice gates and application to discharge measurement, *J Hydraul Eng*, 135 (12) (2009) 1086–1091. http://dx.doi.org/10.1061/(ASCE)HY.1943-7900.0000122

15 Sepúlveda C, Gómez M & Rodellar J, Benchmark of Discharge Calibration Methods for Submerged Sluice Gates, *J Irrig Drain Eng*, 135 (5) (2009) 676–682. http://dx.doi.org/10.1061/(ASCE)IR.1943-4774.0000013

16 Yoosefdoost A & Lubitz W D, Sluice Gate Design and Calibration: Simplified Models to Distinguish Flow Conditions and Estimate Discharge Coefficient and Flow Rate, *Water*, 14 (2022) p. 1215. https://doi.org/10.3390/w14081215

17 Habibzadeh A, Vatankhah A R & Rajaratnam N, Role of Energy Loss on Discharge Characteristics of Sluice Gates, *J Hydraul Eng*, 137 (9) (2011) 1079–1084. http://dx.doi.org/10.1061/(ASCE)HY.1943-7900.0000406

18 Robertson C I & Sellin R H J, A model study of tidal barrage sluices for minimum energy loss, *J Hydraul Res*, 23 (5) (1985) 453–466. http://dx.doi.org/10.1080/00221688509499338

19 Falconer R A, Xia J, Lin B & Ahmadian R, The Severn Barrage and other tidal energy options: hydrodynamic and power output modeling, *Sci China Ser E: Technol Sci*, 52 (11) (2009) 3413–3424. https://doi.org/10.1007/s11431-009-0366-z

20 Xia J, Falconer R A & Lin B, Impact of different operating modes for a Severn Barrage on the tidal power and flood inundation in the Severn Estuary, UK, *Appl Energy*, 87 (7) (2010) 2374–2391. http://dx.doi.org/10.1016/j.apenergy.2009.11.024

21 Zhou J, Falconer R A & Lin B, Refinements to the EFDC model for predicting the hydro-environmental impacts of a barrage across the Severn Estuary, *Renew Energy*, 62 (2014) 490–505. http://dx.doi.org/10.1016/j.renene.2013.08.012

22 Angeloudis A, Falconer R A, Bray S & Ahmadian R, Representation and Operation of Tidal Energy Impoundments in a Coastal Hydrodynamic Model, *Renew Energy*, 99 (2016) 1103–1115. http://dx.doi.org/10.1016/j.renene.2016.08.004

23 Habib M A, Ben-Mansour R, Badr H M & Kabir M E, Erosion and penetration rates of a pipe protruded in a sudden contraction, *Comput Fluids*, 37 (2) (2008) 146–160. https://doi.org/10.1016/j.compfluid.2007.05.002

24 Tong G, Zhang G, Christopher D M, Bjerg B, Ye Z & Cheng J, Evaluation of turbulence models to predict airflow and ammonia concentrations in a scale model swine building enclosure, *Comput Fluids*, 71 (2013) 240–249. http://dx.doi.org/10.1016/j.compfluid.2012.10.020

25 Azimi H & Shabanlou S, Numerical study of bed slope change effect of circular channel with side weir in supercritical flow conditions, *Appl Water Sci*, 8 (6) (2018) p. 166. https://doi.org/10.1007/s13201-018-0816-5

26 Wang Y, Wang W, Hu X & Liu F, Experimental and numerical research on trapezoidal sharp-crested side weirs, *Flow Meas Instrum*, 64 (2018) 83–89. https://doi.org/10.1016/j.flowmeasinst.2018.10.005

27 Laws E M & Ouazanne A K, Compact installations for differential flowmeters, *Flow Meas Instrum*, 5 (2) (1994) 79–85. http://dx.doi.org/10.1016/0955-5986(94)90040-X

28 Hirt C W & Nichols B D, Volume of fluid (VOF) method for the dynamics of free boundaries, *J Comput Phys*, 39 (1) (1981) 201–225.
29 Bhosekar V V, Jothiprakash V & Deolalikar P B, Orifice spillway aerator: hydraulic design, *J Hydraul Eng*, 138 (6) (2012) 563–572. http://dx.doi.org/10.1061/(ASCE)HY.1943-7900.0000548
30 Cozzolino L, Cimorelli L, Covelli C, Morte R D & Pianese D, The analytic solution of the Shallow-Water Equations with partially open sluice-gates: the dam-break problem, *Adv Water Resour*, 80 (2015) 90–102. http://dx.doi.org/10.1016/j.advwatres.2015.03.010
31 Jaeger R, Tondera K, Jacobs C, Porter M & Tindale N, Numerical and physical modeling to improve discharge rates in open channel infrastructures, *Water*, 11 (7) (2019) p. 1414. http://dx.doi.org/10.3390/w11071414
32 Pfister M & Chanson H, Scale Effects in Physical Hydraulic Engineering Models. Discussion, *J Hydraul Res, IAHR*, 50 (2) (2012) 244–246. http://dx.doi.org/10.1080/00221686.2012.654671
33 Wang H, Uys W & Chanson H, Alternative mitigation measures for fish passage in standard box culverts: physical modelling, *J Hydro-environ Res*, 19 (2018) 214–223. http://dx.doi.org/10.1016/j.jher.2017.03.001
34 Xiao Y, Wang W, Hu X & Zhou Y, Experimental and numerical research on portable short-throat flume in the field, *Flow Meas Instrum*, 47 (2016) 54–61. http://dx.doi.org/10.1016/j.flowmeasinst.2015.11.003